# Low Temperature Surface Preparation of GaN Substrates for Atomic Layer Epitaxial Growth: Assessment of Ex-Situ Preparations

Running title: Low Temperature Surface Preparation of GaN Substrates for Plasma Assisted-Atomic Layer Epitaxial Growth

Running authors: Rosenberg et al.


Samantha G. Rosenberg [a)]

American Society of Engineering Education, 1818 N Street N.W. Suite 600, Washington DC 20036, Residing at U.S. Naval Research Laboratory

Daniel J. Pennachio

University California, Santa Barbara, Materials Dept, Santa Barbara, CA 93106

Christa Wagenbach

Department of Physics and Division of Materials Science & Engineering, Boston University, 590 Commonwealth Ave., Boston, Massachusetts 02215

Scooter D. Johnson and Neeraj Nepal,

U.S. Naval Research Laboratory, 4555 Overlook Ave., SW, Washington, DC 20375

Alexander C. Kozen, and Jeffrey Woodward

American Society of Engineering Education, 1818 N Street N.W. Suite 600, Washington DC 20036, Residing at U.S. Naval Research Laboratory

Zachary Robinson

Department of Physics, The College at Brockport SUNY, 350 New Campus Drive, Brockport, New York 14420

Howie Joress

Cornell High Energy Synchrotron Source, Cornell University, Ithaca, NY 14850

Karl F. Ludwig

Department of Physics and Division of Materials Science & Engineering, Boston University, 590 Commonwealth Ave., Boston, Massachusetts 02215

Chris J. Palmstrøm

University California, Santa Barbara, Materials Dept and Dept. of Electr. and Comp. Eng., Santa Barbara, CA 93106

Charles R. Eddy, Jr.

U.S. Naval Research Laboratory, Power Electronics Materials, 4555 Overlook Ave., SW, Washington, DC 20375

[a)] Electronic mail: Samantha.rosenberg.ctr@nrl.navy.mil

*In-situ* and *in-vacuo* surface studies of *in-situ* and *ex-situ* GaN substrate preparation were conducted to advance fundamental understanding of GaN surface preparation for low temperature atomic layer epitaxial growth. Grazing incidence small angle x-ray scattering (GISAXS) information is complemented with *in-vacuo* x-ray photoelectron spectroscopy and *ex-situ* atomic force microscopy studies to assess different *ex-situ* sample preparation methods to produce the most suitable GaN surface for epitaxy. We have determined that a UV-ozone exposure followed by an HF dip produces the cleanest and smoothest GaN surface. We have further determined with GISAXS that subjecting the optimum surface to our established low temperature emulated gallium flash-off atomic level process (GFO ALP) eliminates the need for any nitridation ALP. These *ex-situ* and *in-situ* cleaning preparations result in clean, highly-ordered surfaces that should provide an ideal substrate for high quality crystalline epitaxial films.

# I. INTRODUCTION

Low temperature plasma-assisted atomic layer epitaxy (ALEp) can be used to grow aluminum nitride (AlN) and indium nitride (InN) for various applications.[1–6] The materials grown using ALEp have shown good crystalline quality, but exhibit unacceptable levels of carbon incorporation and have been grown mostly on sapphire.[1] GaN is not only a better lattice match to AlN and InN than sapphire, but also offers better thermal properties than sapphire, leading to its popularity in high power devices.[7–13] These properties motivate us to develop growth of ALEp materials on GaN substrates.

However, bulk GaN substrate technology is far less mature than sapphire, leading to the need to determine the best preparation method for a pristine starting surface that will promote epitaxy. In the GaN molecular beam epitaxy community recent studies show that a combination of *ex-situ* wet chemical etches followed by an *in-situ* clean of some kind produces the optimal result for GaN substrates.[12,13] During metal-organic chemical vapor deposition (MOCVD) growth, GaN surfaces are cleaned by exposure to high temperatures and overpressures of nitrogen or ammonia,[14] however due to the low temperature nature of the ALEp processes, alternative low temperature methods of cleaning the surface, both *ex-situ* and *in-situ* are needed. N. Nepal *et.al.* has previously shown promising results with a piranha etch to prepare GaN surfaces for atomic layer deposition (ALD) oxide deposition, however that etch resulted in some oxide remaining on the surface, reducing its suitability for nitride epitaxy.[15] C. English *et. al.* conducted an in-depth study of *ex-situ* GaN surface preparations before ALD deposition of high-κ dielectrics, where piranha was again assessed to produce optimum results.[16] However both of these studies were for oxide deposition and concluded that a small layer of oxygen on the GaN surface was benificial.

Therefore, in this study we explored wet chemical etch procedures with the aim of cleaning the surface of not only carbon, but oxygen as well.

In this work, we employ *in-vacuo* XPS methods to assess surface carbon and oxygen levels after *ex-situ* chemical treatments. We investigate the surface smoothness of the substrates using both AFM and grazing incidence small angle x-ray scattering (GISAXS). GISAXS an *in-situ* technique that has previously been useful in elucidating the growth mechanism for AlN and InN on sapphire,[5,6] will be used here to assess our *in-situ* cleaning technique, an emulated gallium flash-off (GFO) atomic level process (ALP) on our *ex-situ* treated GaN substrates.[17] Using these surface science techniques, we strive to develop a fundamental understanding of the cleaning processes for an optimal GaN starting surface for ALEp.

# II. EXPERIMENTAL

Two identical sets of experiments were performed in separate systems. One in a custom-built multicomponent UHV system with a base pressure of ~$10^{-10}$ Torr, which permitted *in-vacuo* XPS studies and the other in a custom-built hot wall (150°C), ALEp reactor with a base pressure of 2.6 x $10^{-2}$ Torr, which permitted *in-situ* studies of surface morphological evolution in real-time at the G3 beamline at Cornell High Energy Synchrotron Source (CHESS)[5,6,17]. The following experimental section outlines the preparation for both studies unless otherwise explicitly stated.

## *A. Ex-situ Sample Preparation*

Hydride vapor phase epitaxy (HVPE) bulk GaN substrates (Kyma and Lumilog) were diced into ~1 $cm^2$ squares. Kyma substrates were semi-insulating, 488 μm thick, and had a 0.73° offcut, while the Lumilog substrates were N-type, 300 μm thick, and a 0.5°

offcut. They were prepared by first swirling them in acetone, isopropanol, and then DI (~18 MΩ-cm) water for 5 min each. Each substrate was then blown dry with pure nitrogen gas generated from liquid nitrogen boil-off. Following solvent cleaning, each substrate square was then processed using one of the following wet chemical etches followed by a subsequent DI water rinse and $N_2$ blow dry: a) 5 min in 10 % HF solution ACS grade (CAS number: 7664-39-3); b) 1 min in 10% HCl solution ACS grade (CAS number: 7647-01-0); c) 10 min in 1:5 $H_2O_2$:$H_2SO_4$ (piranha solution) at 80°C; d) 10 min in 1:5 $H_2O_2$:$H_2SO_4$ (piranha solution) at 80°C and then rinsed in DI and dried followed by 1 min in concentrated (48 %) HF and then rinsed and dried as above; e) 10 min in a Samco UV-1 UV-ozone instrument in a clean room, transported back to the lab after ozone oxidation, and etched for 1 min in concentrated (48 %) HF then rinsed and dried as above. For XPS studies, the substrate was then held in place on a Ta sample platen by spot-welded Ta foil, placed into the load lock of the experimental set up, then pumped down for load-in. This weld and load-in procedure was completed in under ~20 minutes. For GISAXS studies, the substrates were mounted onto the sample platen using tantalum clips, with care to ensure the greatest interaction area for the x-ray beam and to avoid any macro-defects in the substrate, and loaded into the vacuum chamber in under ~15 minutes. For AFM studies, the samples were extracted from the UHV chamber after XPS and adhered to an isolation table with a vacuum chuck.

## *B. Emulated Gallium Flash-Off Atomic Level Process*

The previously reported emulated gallium flash-off (GFO) atomic level process (ALP) was performed directly after our *ex-situ* cleaning and once the substrate temperature had equilibrated.[1,17] These optimal results, namely 10 cycles of the GFO ALP at 500°C,

were used for this study. The GFO ALP is a 60 second cycle consisting of a 60 millisec pulse of trimethylgallium, 10 second Ar purge, 30 second $H_2$ plasma exposure at 300 W forward power and 75 sccm flow rate. Pressure in the custom-built reactor during the temperature ramp was 6.2 x $10^{-2}$ Torr under flowing, purified argon. Note that while the substrate temperature was equilibrating at the synchrotron, the x-rays were concurrently aligned to the sample and the detector. For our custom-built reactor, we estimate a substrate temperature uncertainty of ± 20°C, measured with our Williamson Pro40 model pyrometer.

At the synchrotron, after 10 cycles of GFO ALP, 10 cycles of a $H_2$ plasma clean, henceforth refered to as hydrogen clean ALP, followed by 10 cycles of a $N_2$ plasma clean, henceforth refered to as nitridation ALP, were executed at the GFO ALP temperature. These two processes are previously described elsewhere for the cleaning of sapphire substrates for ALEp.[5,6,17] It should be noted that the hydrogen clean and nitridation ALPs are legacy processes from previous ALEp growth on sapphire that required surface nitridation to promote growth.

## C. Characterization Methods

### 1. In-situ Methods: Grazing Incidence Small Angle X-ray Scattering

A custom-built stainless steel reactor, previously described,[5,6,17] was used at the Cornell High Energy Synchrotron Source (CHESS) G3 beamline to monitor surface morphological evolution during processing using *in-situ* grazing incidence small angle x-ray scattering (GISAXS). A diffuse scatting pattern was created from an X-ray beam with a 0.8° angle of incidence. Scattered X-rays were collected every second using a 2D Dectris 2M Pilatus detector positioned at 0.2° relative to the sample surface plane. The area

detector captures the scattering distribution between the critical angle where the Yoneda wing appears, and the specular reflection. Two sets of experiments were performed using GISAXS: the X-ray energy for first set of experiments was 11.22 keV, while the energy for the second set was 10.18 keV. Reducing the X-ray energy below the Ga flourecence threshold decreased the background scattering intensity, increasing signal-to-noise ratio of our measurements, without effecting the process. Additional experimental details have been described previously.[5,6,17]

## 2. *In-vacuo Methods: X-ray Photoelectron Spectroscopy*

In the custom-built UHV system, after the load-lock had reached a sufficient pressure (~$1x10^{-6}$), the samples were transferred to a preparation chamber with base pressure ~$10^{-10}$ Torr and outgassed at 400°C for 90 minutes. No additional *in-vacuo* preparation steps were taken prior to XPS analysis. Samples were transferred *in-vacuo* to a Surface Science Laboratory SSX-100 XPS with a monochromatic Al-$K_\alpha$ source at a 55˚ photoelectron emission angle. A pass energy of 151 eV was used for the survey scan and composition analysis, while a pass energy of 24.54 eV was used for position analysis of the individual elements. For all samples, a low-energy electron flood gun was utilized during XPS acquisition to reduce charging effects that may occur from the GaN substrate. Using CASA, GaN samples were manually aligned to the Ga ($2p_{3/2}$) peak at 1117.8 eV.[18] In addition, a GaMn calibration sample was created and measured, *in-vacuo*, using a MOD Gen-II EMOF MBE system so that the Ga Auger peaks could be separated from both the nitrogen (1s) and the oxygen (1s) spectra. CasaXPS software was used for all fitting and analysis of XPS spectra.

## 3. *Ex-situ Methods*

An Asylum Research MFP-3D AFM system using setpoints between 400 to 700 mV in tapping mode, in air, was used to examine the surface of the substrates after the various *ex-situ* cleans and XPS analysis were performed. The noise floor of the AFM is 0.03 nm when the cantilever is engaged with the sample surface. The substrates were taken out of the UHV system and transported to the AFM for imaging, resulting in atmospheric exposure. Gwyddion software was used to process and analyze the images.[19] A mean plane subtraction followed by a median alignment and a correction for horizontal scars were applied to all images before statistical analysis.[19]

# III. RESULTS AND DISCUSSION

## *A. Ex-situ Results and In-situ Results*

Figure 1 shows AFM images with their respective RMS roughness values for Kyma GaN substrates a) as received, b) after the 10 % HF etch as described in the experimental section, c) after the 10 min piranha etch, d) after the 10 min piranha etch followed by the 1 min concentrated HF etch and e) after at 10 min UV-ozone treatment followed by a 1 min concentrated HF etch. AFM of the bare (unprocessed) Kyma substrates shows that there is some roughness on a generally disordered surface of the as-received substrates, which is to be expected from the immature technology of the chemical and mechanical polishing (CMP) that the substrates go through before they are shipped. The bare Kyma has a RMS roughness value of 0.44 nm. Figure 1 (b) shows that after the 10% HF etch there is still roughness on the surface. In addition, the RMS roughness value has increased to 0.75 nm after the treatment. Figure 1(c) shows that the piranha etch removes a lot of the particles on the surface, however they are now larger in size and the RMS roughness value is now closer to what the bare Kyma substrate was as received, 0.48 nm. Figure 1(d) shows

that the piranha etch followed by concentrated HF reveals a stepped GaN surface and a RMS roughness value of 0.11 nm. Figure 1 (e) shows that after the UV-ozone followed by concentrated HF etch also reveals the stepped GaN surface and a RMS roughness value of 0.09 nm.

Figure 2 shows AFM images with their respective RMS roughness values for Lumilog GaN substrates a) as received, b) after the 10 min piranha etch followed by the 1 min concentrated HF etch and c) after at 10 min UV-ozone treatment followed by a 1 min concentrated HF etch. Figure 2 (a) shows the as received Lumilog has particles on a generally disordered surface, consistent with current CMP methods and a substrate exposed to atmosphere without any cleaning. The RMS roughness value for as-received Lumilog is 0.52 nm. Figure 2 (b) shows that after the piranha and concentrated HF etch the stepped surface of the GaN substrate is revealed. The RMS roughness value is 0.08 nm. Figure 2(c) shows that after UV-ozone and concentrated HF etch also reveals the stepped surface of the GaN substrate. The RMS roughness value is 0.15 nm.

Table 1 shows the XPS results of the percentage of carbon, oxygen and remaining impurities found on the surface of the substrates, as well as the RMS roughness numbers from the AFM analysis above. Both the Kyma and Lumilog GaN had large pits on the surface allowing for etchant to remain trapped on the surface if the DI rinse was not thorough. This trapping is the proposed source of impurities in the samples. Optimization of the DI rinse was attempted, but aggressive sonication or rough handling resulted in substrate fracture, limiting the success of more aggressive rinses. Also note that XPS analysis assumes a continuous film on the surface, but the contamination may not always take this form, so the amount of carbon and oxygen is typically overestimated in the

reported cases. The XPS results also include a small contribution coming from the substrate bulk and not just from the surface, as XPS probes the top ~10 nm of the sample on average, depending on the composition. HCl treatment resulted in the highest amount of carbon retained on the surface of the GaN substrate and, as this is undesirable, no further characterization was performed on such samples. 10% HF also results in a high percentage of carbon remaining on the surface. The piranha etch seems to reduce carbon past the detection limits of the XPS, but results in a high amount of oxygen on the surface, as expected from an oxidative method. The UV-ozone followed by concentrated HF etch shows a difference between the Kyma and Lumilog GaN samples, but both substrates show a reduction in carbon and oxygen compared to preceding etch methods. The piranha and concentrated HF etch on Kyma also shows a reduction in both carbon and oxygen. The piranha and concentrated HF treatment on Lumilog XPS results is an average of two data points as the sample broke during transfer and both pieces of the substrate were analyzed with XPS. The results were averaged, but we attribute the higher percentage of carbon and oxygen to the fracturing event. Based on the XPS and AFM results, we have downselected our samples for the GISAXS studies and only processed the two etches that gave us the best results: piranha with subsequent concentrated HF etch and UV-ozone with subsequent concentrated HF etch.

Table 1. XPS relative elemental composition of C, O, impurities and RMS roughness found after etching Kyma (K) and Lumilog (L) GaN substrates.

| ***Ex-Situ* Clean** | **Carbon** | **Oxygen** | **Impurity** | **RMS** |
|---|---|---|---|---|
| Bare (K) | -- | -- | -- | 0.44 nm |
| HCl (K) | 17.9 % | 9.9 % | ~1 % Cl | -- |

| | | | | |
|---|---|---|---|---|
| 10% HF (K) | 10.4 % | 6.7 % | -- | 0.75 nm |
| Piranha (K) | ~1 % | 9.9 % | ~1 % S | 0.48 nm |
| UV-ozone +HF (K) | 1.6 % | 5.5 % | ~1 % F | 0.09 nm |
| Piranha +HF (K) | 2.1 % | 5.5 % | ~1 % F | 0.11 nm |
| Bare (L) | -- | -- | -- | 0.52 nm |
| UV-ozone +HF (L) | 4.5 % | 6.0 % | -- | 0.15 nm |
| Piranha +HF (L)* | 3.4 % | 8.3 % | ~1 % F | 0.08 nm |

## *B. In-situ GISAXS Results*

Figure 3 shows contour plots for the GFO ALP during the entire 10 cycles conducted after the (a) piranha and concentrated HF etch and (b) UV-ozone and concentrated HF on Lumilog GaN substrates only. These plots of real-time GISAXS intensity over time, display the evolution of scattering in $q_y$ ($nm^{-1}$). The GFO process is delayed for the first ~56 seconds to provide a baseline for all subsequent GISAXS plots. Scattering intensity was normalized to the upstream incident x-ray intensity recorded concurrently with the experiment. For GISAXS results the integrated intensity is directly proportional to the mean squared roughness.[20,21] Figure 3(a) shows an increased and uniform intensity for the GFO ALP method when applied to surfaces cleaned with piranha and concentrated HF. Figure 3(b) shows a sharp increase in intensity when the GFO ALP

method starts, indicating roughening of the surface, but then a decrease in intensity around 350 seconds, indicating smoothening of the surface, when applied to a surface cleaned with UV-ozone and concentrated HF. The marked difference here in GISAXS results, a smoothening result, allowed us to make a further determination that the UV-ozone/HF preparation is the better of the two.

Having determined that UV-ozone followed by concentrated HF is the best *ex-situ* preparation method from our GISAXS studies, we only continued our experiments on GaN cleaned using this procedure. Figure 4 shows the contour plots for (a) the hydrogen clean ALP and (b) the nitridation ALP which were applied to the GaN substrate after an UV-ozone and concentrated HF *ex-situ* preparation and the GFO ALP were completed. Figure 4 (a) shows that the intensity starts and ends at the same level for the hydrogen clean ALP. Although, the intensity does lower during the 10 cycles, the scattering intensity returns to the baseline level, indicating that the hydrogen clean ALP is not doing any damage to the surface. In contrast, Figure 4 (b) shows a large increase in intensity, and therefore roughness, once the nitridation ALP starts which remains throughout the process.

Figure 5 shows intensity over time at specific $q_y$ values taken from the data used to create the contour plots in Figure 4 which correspond to four approximately horizontal lines in that figure. Four specific $q_y$ were selected to represent a variety of length scales. Figure 5(a) shows that at $q_y$ equal to 0.125 $nm^{-1}$ (~50.24 nm), the trend shown in the contour plot in Figure 4(a) is the same, namely that intensity and therefore roughness starts at a particular point and then decreases, where we can see the individual cycles, before returning to the same intensity and roughness. Figure 5(b) also shows that at $q_y$ equal to 0.125 $nm^{-1}$ (~50.24 nm), the trend shown in the contour plot in Figure 4(b) is the same,

namely that intensity/roughness increases drastically in the first cycles of the nitridation ALP and remains high over the length of the nitridation ALP.

## C. Discussion

The results from Figures 1 & 2 along with Table 1, have shown us that our previous legacy method[17] of cleaning GaN substrates in 10% HF is not the most effective method for removing the carbon and oxygen on the surface of the as-received GaN. In addition, the results show us that while there is some variability in the carbon between the two vendors, Kyma and Lumilog, the substrates are very similar and react similarly to the etching process. Through AFM and XPS studies of the *ex-situ* processes we were able to down select (1) piranha and concentrated HF and (2) UV-ozone and concentrated HF as the two best *ex-situ* preparation methods of GaN substrates for our ALE applications.

These two *ex-situ* cleans were employed as starting points for the *in-situ* synchrotron studies. Figure 3 (a) shows that while the GFO ALP is in progress for the piranha-HF treated surface there is an increase in uniform scattering intensity, correlating to an increase in uniform roughness occurring at all length scales over the substrate. In contrast, Figure 3 (b) for the UV-$O_3$-HF treated surface, shows an initial increase, followed by a decrease in intensity and roughness indicating a smoother GaN substrate at the end of the process which is typically preferred for epitaxy. We hypothesize that this roughening corresponds to removal of the remaining carbon and oxygen left on the surface and potentially some of the GaN substrate material (see Table 1 results), creating a beneficial surface on which to grow. From this experiment we conclude that UV-ozone followed by concentrated HF is a better *ex-situ* preparation method. Studies are underway to track the carbon and oxygen content on the GaN surface after the GFO ALP with XPS.

Having concluded that UV-ozone followed by concentrated HF is best, we continued with our standard *in-situ* preparation of the surface as seen in Figures 4 & 5. Figures 4 & 5 (a) show the hydrogen clean ALP has no additional effect on the surface of the GaN substrate that has received this particular combination of *ex-situ* and *in-situ* preparations. We come to this conclusion because the total scattered intensity starts and ends at the same magnitude. In addition, during the ALP pulse cycles, seen in Figure 5 (a), the intensity also returns to the baseline before another cycle starts, indicating that the hydrogen clean ALP has transformed the surface completely in the view of the x-rays before another cycle can begin, but we are neither roughening or smoothening the surface with this process.

In contrast, Figures 4 & 5 (b) show the nitridation ALP increases substrate roughness, and therefore is not beneficial. As noted in the experimental section, the nitridation ALP is a holdover from when we used to grow on sapphire and a nitrogen rich surface was not readily available and had to be artificially created. However, with a GaN substrate, that is not the case. On the basis of these results we therefore no longer use this process.

# IV. SUMMARY AND CONCLUSIONS

This work has assessed a collection of *ex-situ* cleaning methods for GaN substrates using XPS and AFM. Two optimum processes are identified, and the resulting surfaces are further studied, using real-time GISAXS, during an optimized set of *in-situ* ALPs including a GFO, hydrogen clean and nitridation. AFM and XPS results indicate that either piranha followed by concentrated HF or UV-ozone followed by concentrated HF result in the best *ex-situ* preparation method for GaN. However, after looking at the *in-situ* GISAXS

results, superior surfaces result from UV-ozone followed by concentrated HF due to the fact that the GFO ALP is able to roughen and then smooth the surface creating a useful epi-ready surface. In addition, it seems that after using the GFO ALP on the GaN substrate, an empirical nitridation ALP degrades the surface and, therefore, should not be used in low temperature preparation of GaN surfaces for low temperature atomic layer epitaxy.

## ACKNOWLEDGMENTS

Research conducted at the U.S. Naval Research Laboratory was supported by the Office of Naval Research. Research conducted at University California Santa Barbara was funded by the Laboratory University Collaboration Initiative (LUCI) program and the Vannevar Bush Faculty Fellowship [N00014-15-1-2845], which were sponsored by the Basic Research Office, Office of Undersecretary of Defense for Research & Engineering. The authors would like to acknowledge Dr. Arthur Woll of CHESS, without his help this work would not have been possible. Experiments conducted at CHESS were supported by the National Science Foundation and the National Institutes of Health/National Institute of General Medical Sciences under NSF award DMR-1332208. The authors would also like to acknowledge Austin Hickman for his help in sample preparation. The authors would like to thank the developers of ImageJ and Gwyddion. S.G. Rosenberg, J. Woodward, and A. C. Kozen would also like to acknowledge the support of the American Society for Engineering Education and U.S. Naval Research Laboratory postdoctoral fellowship program. D.J. Pennachio would like to acknowledge support by the Department of Defense (DoD) through the National Defense Science & Engineering Graduate Fellowship (NDSEG) Program. The Boston University component of this work was supported by the National Science Foundation (NSF) under Grant No. DMR-1709380.

[1] N. Nepal, S.B. Qadri, J.K. Hite, N.A. Mahadik, M.A. Mastro, and C.R. Eddy, Appl. Phys. Lett. **103**, (2013).

[2] C.R. Eddy, N. Nepal, J.K. Hite, and M.A. Mastro, J. Vac. Sci. Technol. A Vacuum, Surfaces, Film. **31**, 058501 (2013).

[3] R.S. Pengelly, S.M. Wood, J.W. Milligan, S.T. Sheppard, and W.L. Pribble, IEEE Trans. Microw. Theory Tech. **60**, 1764 (2012).

[4] N. Nepal, V.R. Anderson, J.K. Hite, and C.R. Eddy, Thin Solid Films **589**, 47 (2015).

[5] N. Nepal, V.R. Anderson, S.D. Johnson, B.P. Downey, D.J. Meyer, A. DeMasi, Z.R. Robinson, K.F. Ludwig, and C.R. Eddy, J. Vac. Sci. Technol. A Vacuum, Surfaces, and Film. **35**, 031504 (2017).

[6] V.R. Anderson, N. Nepal, S.D. Johnson, Z.R. Robinson, A. Nath, A.C. Kozen, S.B. Qadri, A. DeMasi, J.K. Hite, K.F. Ludwig, and C.R. Eddy, J. Vac. Sci. Technol. A Vacuum, Surfaces, Film. **35**, 031508 (2017).

[7] D.J. Meyer, D.A. Deen, D.F. Storm, M.G. Ancona, D. Scott Katzer, R. Bass, J.A. Roussos, B.P. Downey, S.C. Binari, T. Gougousi, T. Paskova, E.A. Preble, and K.R. Evans, IEEE Electron Device Lett. **34**, 199 (2013).

[8] P. Kruszewski, P. Prystawko, I. Kasalynas, A. Nowakowska-Siwinska, M. Krysko, J. Plesiewicz, J. Smalc-Koziorowska, R. Dwilinski, M. Zajac, R. Kucharski, and M. Leszczynski, Semicond. Sci. Technol. **29**, (2014).

[9] E. Frayssinet, W. Knap, P. Lorenzini, N. Grandjean, J. Massies, C. Skierbiszewski, T. Suski, I. Grzegory, S. Porowski, G. Simin, X. Hu, M.A. Khan, M.S. Shur, R. Gaska, and D. Maude, Appl. Phys. Lett. **77**, 2551 (2000).

[10] D.F. Storm, D.J. Meyer, D.S. Katzer, S.C. Binari, T. Paskova, E.A. Preble, K.R. Evans, L. Zhou, and D.J. Smith, J. Vac. Sci. Technol. B, Nanotechnol. Microelectron. Mater. Process. Meas. Phenom. **30**, 02B113 (2012).

[11] I.C. Kizilyalli, A.P. Edwards, O. Aktas, T. Prunty, and D. Bour, IEEE Trans. Electron Devices **62**, 414 (2015).

[12] D.F. Storm, T.O. McConkie, M.T. Hardy, D.S. Katzer, N. Nepal, D.J. Meyer, and D.J. Smith, J. Vac. Sci. Technol. B, Nanotechnol. Microelectron. Mater. Process. Meas. Phenom. **35**, 02B109 (2017).

[13] D.F. Storm, M.T. Hardy, D.S. Katzer, N. Nepal, B.P. Downey, D.J. Meyer, T.O. McConkie, L. Zhou, and D.J. Smith, J. Cryst. Growth **456**, 121 (2016).

[14] S.W. King, J.P. Barnak, M.D. Bremser, K.M. Tracy, C. Ronning, R.F. Davis, and R.J. Nemanich, J. Appl. Phys. **84**, 5248 (1998).

[15] N. Nepal, N.Y. Garces, D.J. Meyer, J.K. Hite, M.A. Mastro, and C.R. Eddy, Appl. Phys. Express **4**, 2 (2011).

[16] C.R. English, V.D. Wheeler, N.Y. Garces, N. Nepal, A. Nath, J.K. Hite, M.A. Mastro, and C.R. Eddy, J. Vac. Sci. Technol. B, Nanotechnol. Microelectron. Mater. Process. Meas. Phenom. **32**, 03D106 (2014).

[17] S.G. Rosenberg, C. Wagenbach, V.R. Anderson, S.D. Johnson, N. Nepal, A.C. Kozen, J.M. Woodward, Z.R. Robinson, M. Munger, K.F. Ludwig, and C.R. Eddy, JVSTA **Submitted**, (2018).

[18] 20899 (2000) NIST X-ray Photoelectron Spectroscopy Database, NIST Standard Reference Database Number 20, National Institute of Standards and Technology, Gaithersburg MD, (n.d.).

[19] D. Nečas and P. Klapetek, Cent. Eur. J. Phys. **10**, 181 (2012).

[20] C. Revenant, F. Leroy, R. Lazzari, G. Renaud, and C.R. Henry, Phys. Rev. B - Condens. Matter Mater. Phys. **69**, 1 (2004).

[21] G. Ozaydin-Ince and K.F. Ludwig, J. Phys. Condens. Matter **21**, (2009).

Figure 1. AFM images of Kyma HVPE GaN substrates (a) as received, (b) after 10 % HF etch, (c) after piranha etch, (d) after piranha and concentrated HF etch, and (e) after UV-ozone and concentrated HF etch.

Figure 2. AFM images of Lumilog HVPE GaN substrates (a) as received, (b) after piranha and concentrated HF etch, and (c) after UV-ozone and concentrated HF etch.

Figure 3. Real-time GISAXS of 10 cycles of GFO ALP on Lumilog HVPE GaN substrates (a) after piranha and concentrated HF etch, and (b) after UV-ozone and concentrated HF etch.

Figure 4. Real-time GISAXS of (a) 10 cycles of hydrogen clean ALP and (b) nitridation ALP on a Lumilog HVPE GaN substrate after a UV-ozone and concentrated HF etch, followed by 10 cycles of GFO ALP.

Figure 5. Real-time GISAXS of (a) 10 cycles of hydrogen clean ALP and (b) nitridation ALP on a Lumilog HVPE GaN substrate after a UV/ozone and concentrated HF etch, followed by 10 cycles of GFO ALP shown through four different $q_y$ values.

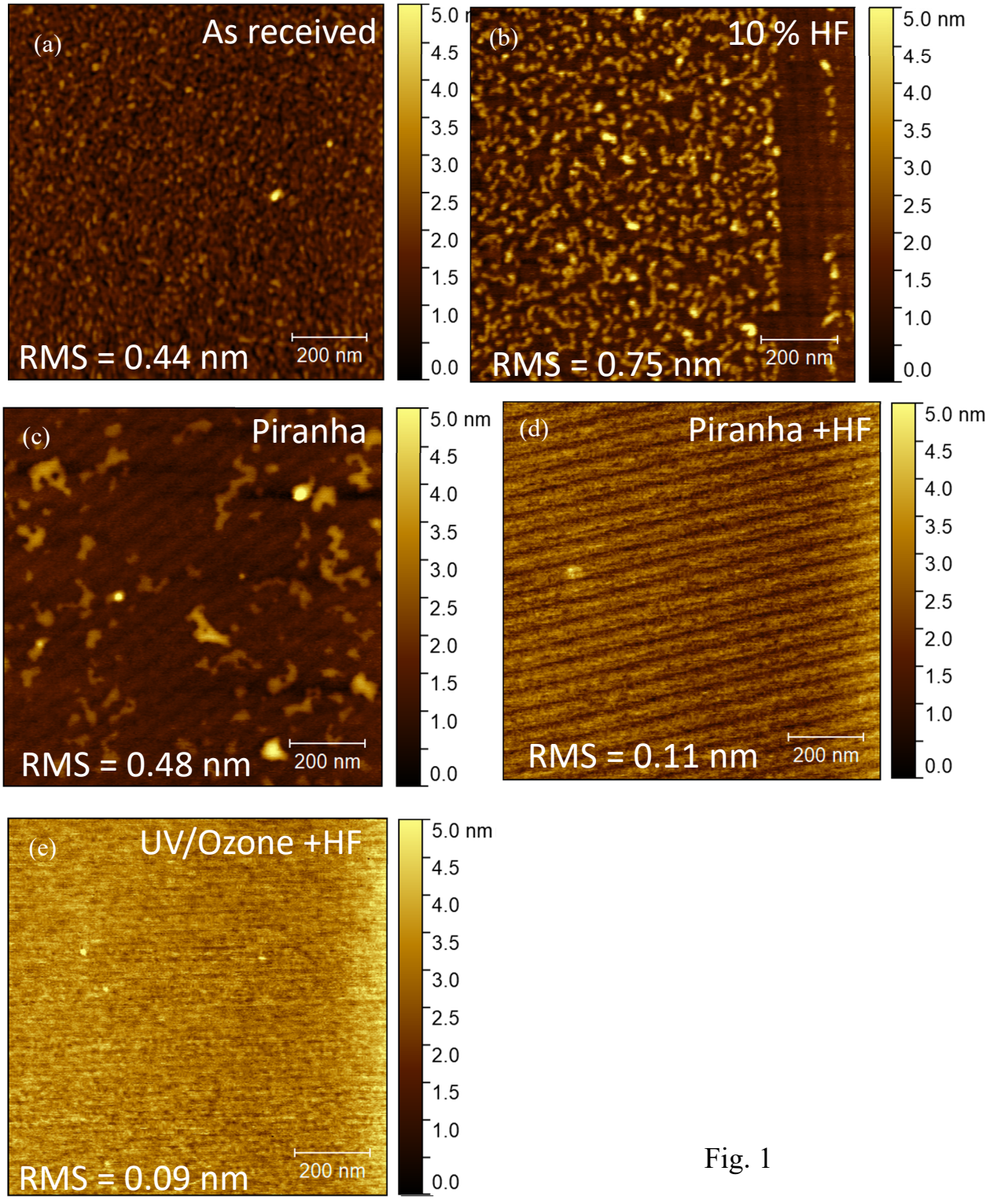
(a)
As received
RMS = 0.44 nm
200 nm
(b)
10 % HF
RMS = 0.75 nm
200 nm
(c)
Piranha
RMS = 0.48 nm
200 nm
(d)
Piranha +HF
RMS = 0.11 nm
200 nm
(e)
UV/Ozone +HF
RMS = 0.09 nm
200 nm
5.0 nm
4.5
4.0
3.5
3.0
2.5
2.0
1.5
1.0
0.0

Fig. 1

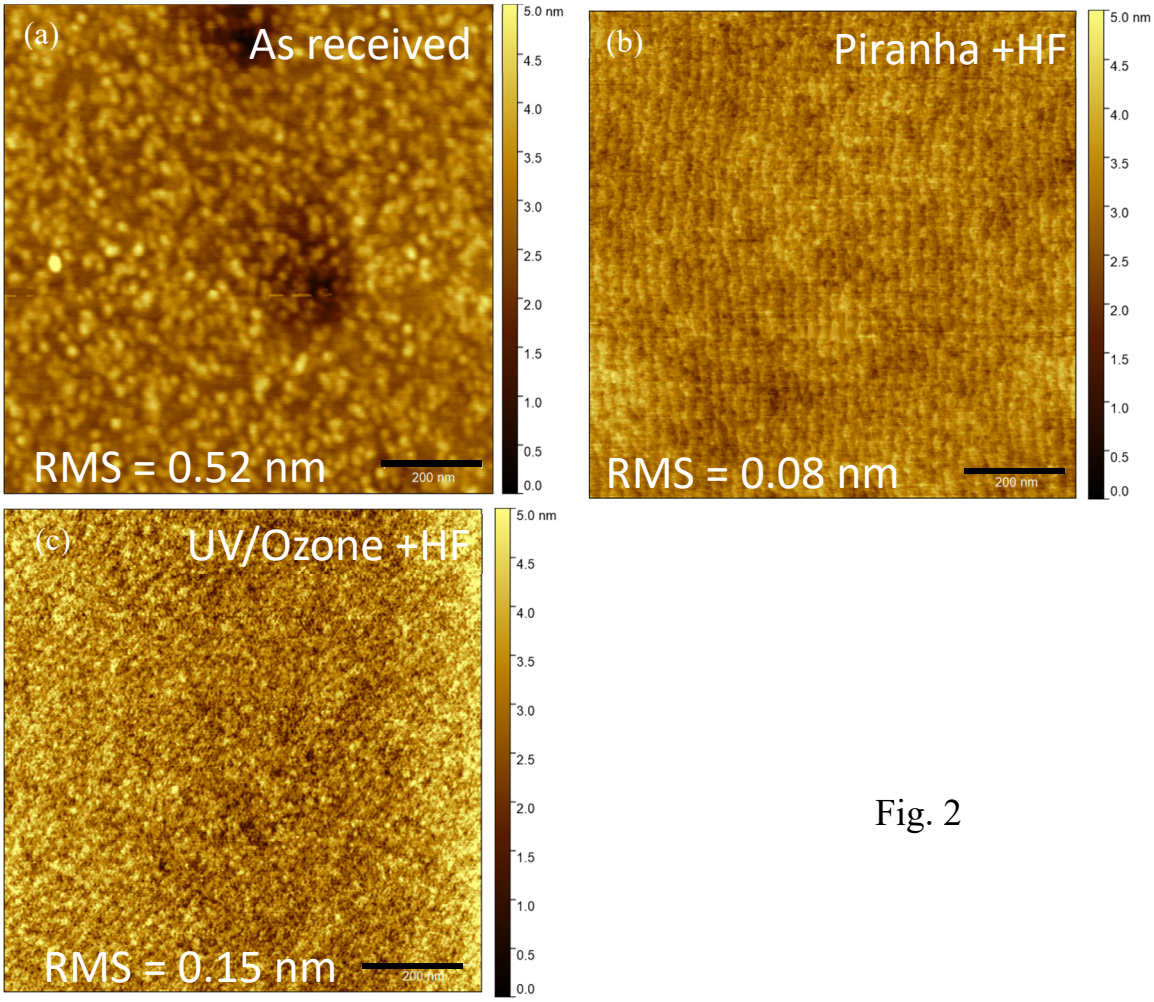
(a)
As received
RMS = 0.52 nm
200 nm
(b)
Piranha +HF
RMS = 0.08 nm
200 nm
(c)
UV/Ozone +HF
RMS = 0.15 nm
200 nm
5.0 nm
4.5
4.0
3.5
3.0
2.5
2.0
1.5
1.0
0.5
0.0

Fig. 2

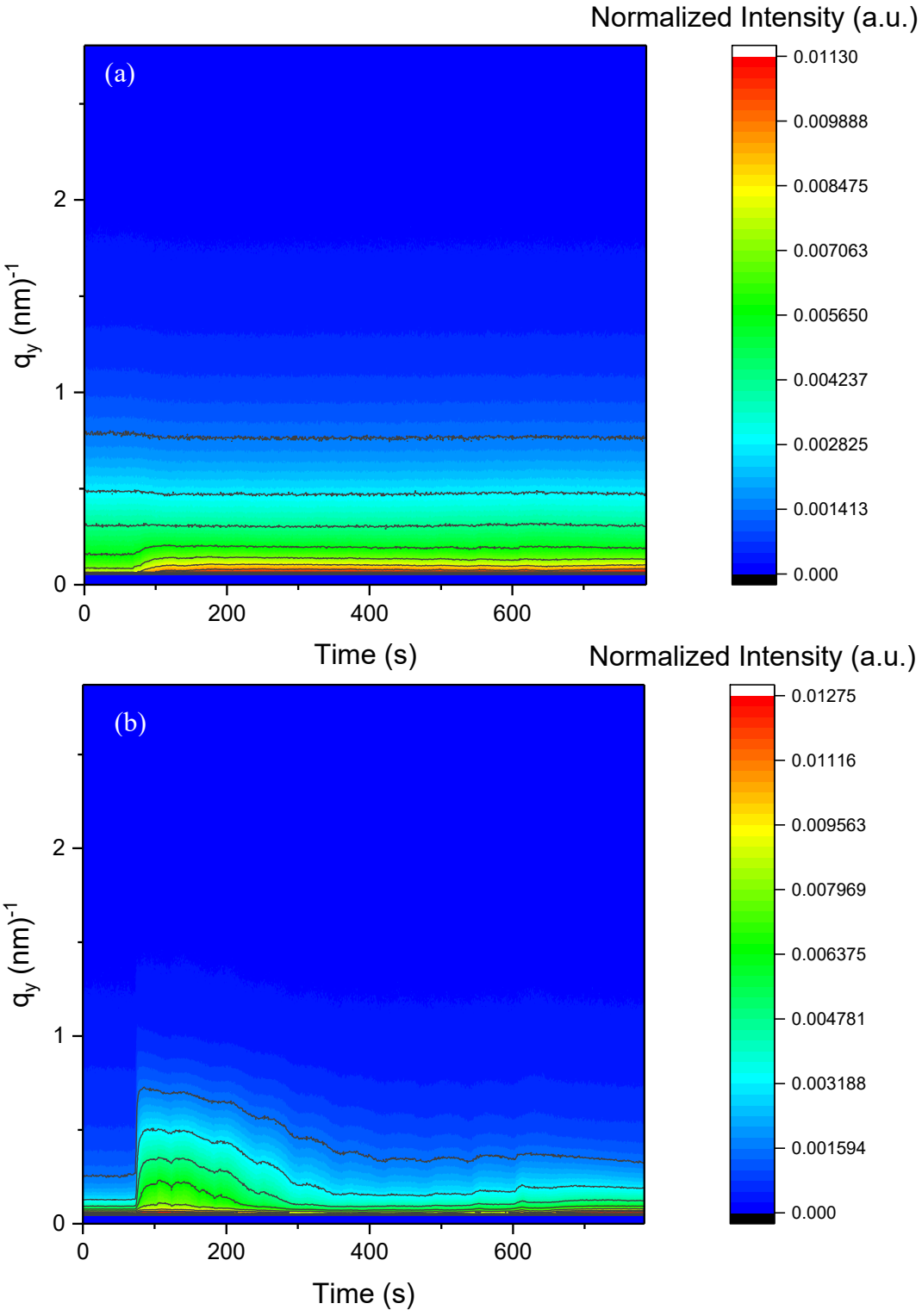
Normalized Intensity (a.u.)
(a)
$q_y$ (nm)$^{-1}$
0
1
2
0
200
400
600
Time (s)
0.01130
0.009888
0.008475
0.007063
0.005650
0.004237
0.002825
0.001413
0.000
Normalized Intensity (a.u.)
(b)
$q_y$ (nm)$^{-1}$
0
1
2
0
200
400
600
Time (s)
0.01275
0.01116
0.009563
0.007969
0.006375
0.004781
0.003188
0.001594
0.000

Fig. 3

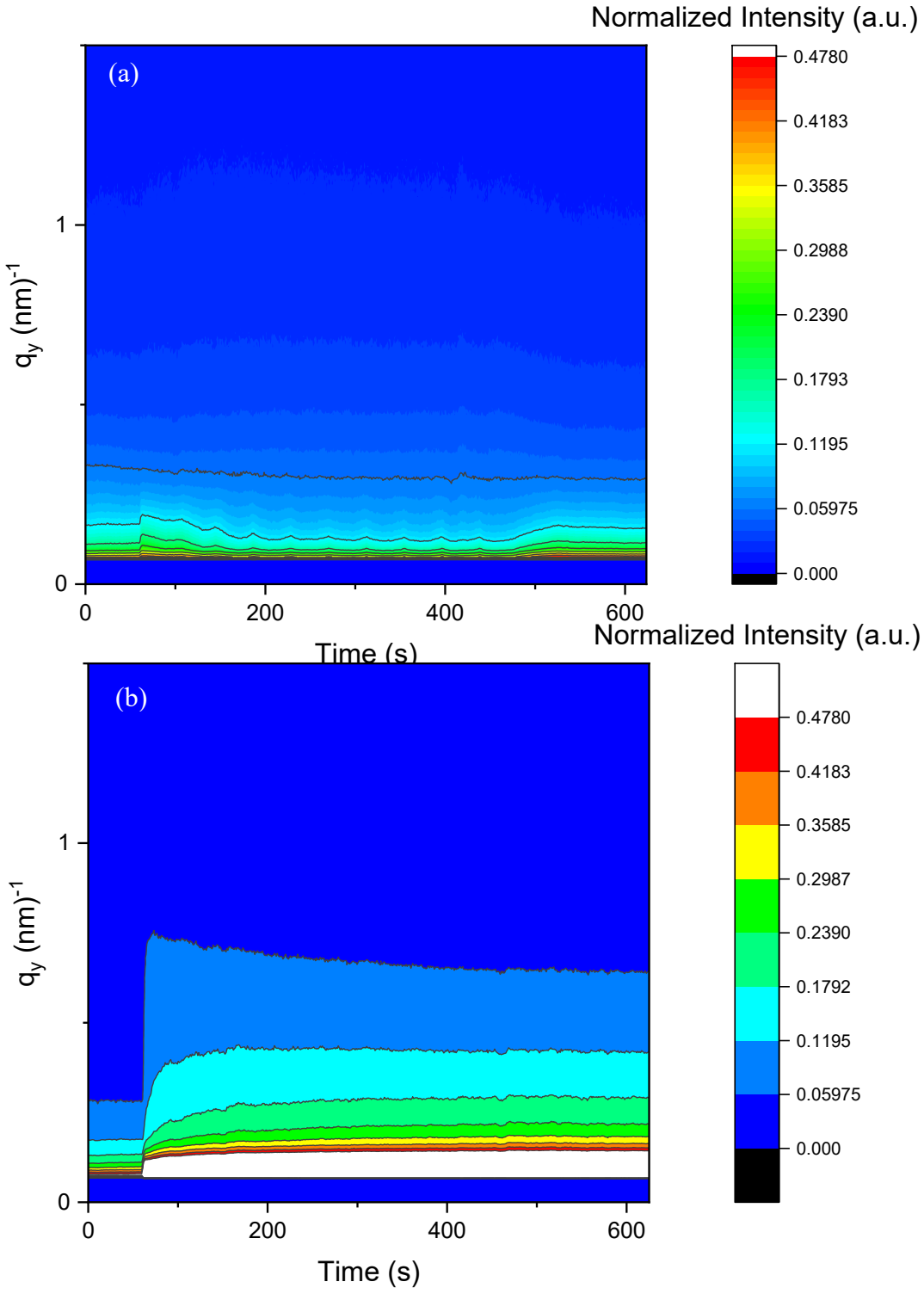
Normalized Intensity (a.u.)
(a)
$q_y$ (nm)$^{-1}$
1
0
0
200
400
600
Time (s)
0.4780
0.4183
0.3585
0.2988
0.2390
0.1793
0.1195
0.05975
0.000
Normalized Intensity (a.u.)
(b)
$q_y$ (nm)$^{-1}$
1
0
0
200
400
600
Time (s)
0.4780
0.4183
0.3585
0.2987
0.2390
0.1792
0.1195
0.05975
0.000

Fig. 4

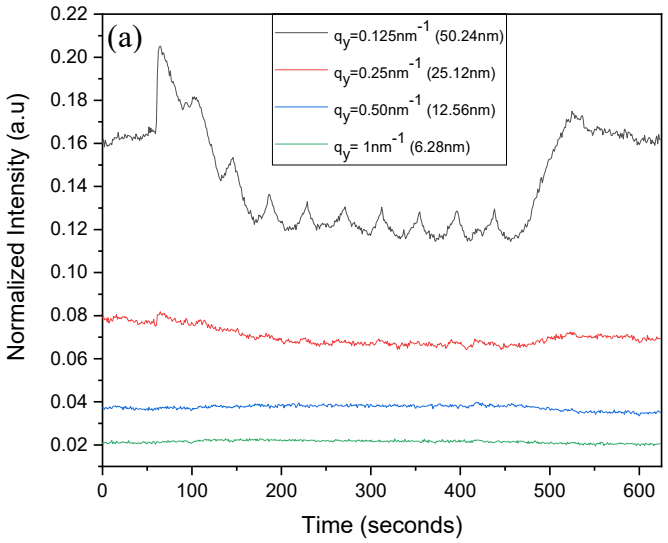
(a)
$q_y$=0.125nm$^{-1}$ (50.24nm)
$q_y$=0.25nm$^{-1}$ (25.12nm)
$q_y$=0.50nm$^{-1}$ (12.56nm)
$q_y$= 1nm$^{-1}$ (6.28nm)
Normalized Intensity (a.u)
Time (seconds)

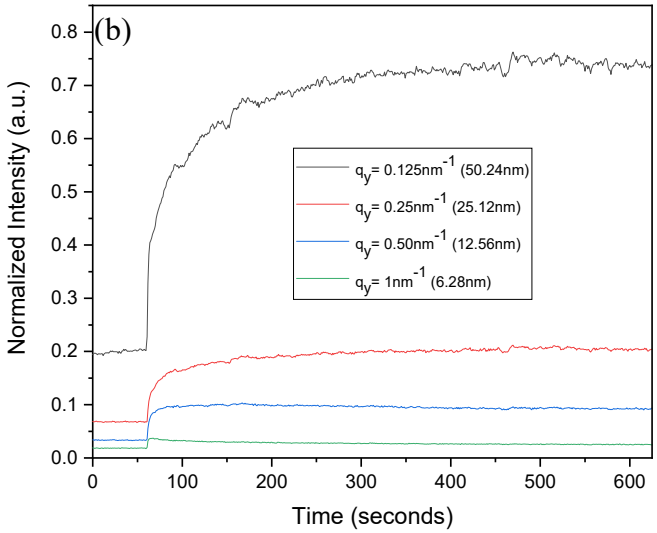
(b)
$q_y$= 0.125nm$^{-1}$ (50.24nm)
$q_y$= 0.25nm$^{-1}$ (25.12nm)
$q_y$= 0.50nm$^{-1}$ (12.56nm)
$q_y$= 1nm$^{-1}$ (6.28nm)
Normalized Intensity (a.u.)
Time (seconds)

Fig. 5